Computational and Applied Mathematics (2020) 39:214
https://doi.org/10.1007/s40314-020-01253-0

A high-order modified finite-volume method on Cartesian grids for nonlinear convection–diffusion problems

Yulong Du[1] · **Yahui Wang**[2,3] · **Li Yuan**[2,3]

Received: 8 October 2019 / Revised: 28 April 2020 / Accepted: 5 July 2020

Abstract

Recently, Buchmüller and Helzel proposed a modified dimension-by-dimension finite-volume (FV) WENO method on Cartesian grids for multidimensional nonlinear conservation laws which can retain the full order of accuracy of the underlying one-dimensional (1D) reconstruction. In this work, we extend this method to multidimensional convection–diffusion equations. The 1D sixth-order central reconstruction of the conserved quantity is utilized for discretizing the diffusion terms in which the diffusion coefficients may be nonlinear functions of the conserved quantity. Using high-order accurate conversions between edge-averaged values and edge center values of any sufficiently smooth quantity, high-order accurate convective and viscous numerical fluxes at cell interfaces are computed. The present modified FV method uses fourth-order accurate conversions for the diffusive fluxes. Numerical examples show that the present method achieves fourth-order accuracy for multidimensional smooth problems, and is suitable for the numerical simulation of viscous shocked flows.

Keywords Finite-volume method · High-order accuracy · Dimension-by-dimension reconstruction · Cartesian grid · Nonlinear convection–diffusion equation

Mathematics Subject Classification 65M08 · 65M12 · 65M20

Communicated by Raphaéle Herbin.

✉ Li Yuan
lyuan@lsec.cc.ac.cn

Yulong Du
kunyu0918@163.com

Yahui Wang
wangyh14@lsec.cc.ac.cn

1 School of Mathematical Sciences, Beihang University, Beijing 100191, People's Republic of China

2 ICMSEC and LSEC, Academy of Mathematics and Systems Science, Chinese Academy of Sciences, Beijing 100190, People's Republic of China

3 School of Mathematical Sciences, University of Chinese Academy of Sciences, Beijing 100190, People's Republic of China

Published online: 14 July 2020

1 Introduction

Convection–diffusion equations are widely used in fluid mechanics, oil reservoir exploration, chemical engineering and many other fields (Morton 1996; Wang et al. 2000; Wang and Li 2007; Lin et al. 2009; Gao et al. 2019; Tian 2019; Huang et al. 2019). Numerical solutions of convection–diffusion equations often use finite difference methods (Chou and Shu 2007; Golbabai and Arabshahi 2010; Sun and Li 2014), finite-volume methods (FVM) (Liang and Zhao 2006; Gao et al. 2019; Tian 2019; Huang et al. 2019; Angermann and Wang 2019) and finite element methods (FEM) (Chana et al. 2014; Cheichan et al. 2019; Zhang and Chen 2019). Due to the merit of local conservation and suitability for complicated domains, FVMs are widely used in engineering computations. FVMs can be applied on structured, unstructured grids or mixed grids. FVMs can also be used on arbitrary Cartesian meshes even those with abrupt changes in mesh sizes and with hanging nodes, without affecting their conservation and accuracy, in contrast to high order FDMs which can only be used on smoothly varying structured meshes. FVMs are easier to implement in the emerging Cartesian Adaptive mesh refinement (AMR) approach (Buchmüller et al. 2016; Tamaki and Imamura 2017; Schmidmayer et al. 2019). This is the main reason that high-order FVMs on Cartesian grids are still under active development.

The finite-volume (FV) weighted essentially non-oscillatory (WENO) methods (Shu 1997) can obtain high-order accurate and essentially non-oscillatory numerical solution for nonlinear conservation laws, thus they were used to solve convection–diffusion equations (Manzini and Russo 2008; Huang et al. 2019) and the Euler and Navier–Stokes equations (Titarev and Toro 2004; Lo et al. 2010; Zhang et al. 2011; Teng et al. 2011; Huang et al. 2019). The simplest and most efficient way to use the FV WENO methods on multidimensional Cartesian grids is to apply the 1D WENO scheme in each direction (Shu 1997). Unfortunately, such a dimension-by-dimension FVM is only second-order accurate for smooth solutions of multidimensional nonlinear hyperbolic conservation laws (Zhang et al. 2011; Buchmüller and Helzel 2014). The conventional high-order FV WENO methods on Cartesian grids use a series of 1D reconstructions to obtain the conserved quantities on quadrature points on cell edges (Titarev and Toro 2004; Zhang et al. 2011; Teng et al. 2011). However, these true FV WENO methods have high computational costs.

Recently, Buchmüller and Helzel (2014) proposed an efficient modified dimension-by-dimension FV WENO method on Cartesian grids which can retain the full order of accuracy of the underlying 1D WENO reconstruction when applied to multidimensional nonlinear hyperbolic conservation laws, and then extended the method to the AMR grid (Buchmüller et al. 2016, 2018). Du et al. (2019) developed a sixth-order modified FV WENO method on 3D Cartesian grids. The key technique in the modified FV WENO method is the conversion between edge-averaged values and edge-center values of the conserved quantity and numerical flux, which makes the modified dimension-by-dimension method achieve the full spatial order of accuracy of the underlying 1D reconstruction. However, extension of the modified FV method to convection–diffusion equations have not been considered. In particular, how to obtain high-order accurate discretizations for a conservative nonlinear diffusion term remains untouched.

In this paper, we extend the modified FV WENO method to multidimensional nonlinear convection–diffusion equations. The main contribution is a fourth-order conversion formula between edge-averaged values and edge-centered values of the viscous fluxes. Numerical results show that the resulting method achieves expected fourth-order accuracy, and is effective in computing convection–diffusion equations. Applications to the compressible Navier–Stokes equations are demonstrated.

The rest of this paper is organized as follows. In Sect. 2, the classical dimension-by-dimension FV diffusion flux is given, which is shown to be only second-order accurate. In Sect. 3, we derive a high-order FV diffusion flux based on the 1D central reconstruction (CR) of the conserved quantity. Then we give the algorithm of the present modified FV method. Numerical results are presented in Sect. 4 to verify the accuracy, efficiency and robustness of the present method. Concluding remarks are given in Sect. 5.

2 Dimension-by-dimension finite-volume method

The fact that the dimension-by-dimension FV WENO method for multidimensional nonlinear hyperbolic conservation laws is only second-order accurate has been shown in Zhang et al. (2011); Buchmüller and Helzel (2014). In this section, we briefly introduce the dimension-by-dimension FV method for a two-dimensional convection–diffusion equation. We will show that the resulting FV diffusive flux with non-constant diffusion coefficients is also only second-order accurate even using a high-order 1D reconstruction.

The two-dimensional convection–diffusion problem considered is given by

$$\begin{aligned} \partial_t u + \nabla \cdot \mathbf{f}(u) - \nabla \cdot \mathbf{f}^{\mathrm{v}}(u, \nabla u) &= s(u, x, y, t), \\ u(x, y, 0) &= u_0(x, y), \end{aligned} \tag{2.1}$$

and proper boundary conditions. Here, $u(x, y, t)$ is the conserved quantity, $\mathbf{f} = \left(f(u),\ g(u)\right)^T$, where $f(u)$ and $g(u)$ are the convective flux functions, $\mathbf{f}^{\mathrm{v}} = \left(f^{\mathrm{v}}(u, \nabla u),\ g^{\mathrm{v}}(u, \nabla u)\right)^T$, where $f^{\mathrm{v}}(u, \nabla u) = a(x, y, u)\partial_x u + b(x, y, u)\partial_y u$ and $g^{\mathrm{v}}(u, \nabla u) = c(x, y, u)\partial_x u + d(x, y, u)\partial_y u$ are the viscous flux functions, and $s(u, x, y, t)$ is the source term. To discretize Eq. (2.1), let $\mathbb{C}_{i,j} = (x_{i-1/2}, x_{i+1/2}) \times (y_{j-1/2}, y_{j+1/2})$ be a control volume in the x-y space, with assumed uniform grid sizes $\Delta x = x_{i+1/2} - x_{i-1/2}$ and $\Delta y = y_{j+1/2} - y_{j-1/2}$.

Integrating Eq. (2.1) over $\mathbb{C}_{i,j}$, we obtain the semi-discrete form of a FV method,

$$\begin{aligned} \frac{\mathrm{d}}{\mathrm{d}t} U_{i,j}(t) = &-\frac{1}{\Delta x}\left(\hat{F}_{i+\frac{1}{2},j} - \hat{F}_{i-\frac{1}{2},j}\right) - \frac{1}{\Delta y}\left(\hat{G}_{i,j+\frac{1}{2}} - \hat{G}_{i,j-\frac{1}{2}}\right) \\ &+\frac{1}{\Delta x}\left(\hat{F}^{\mathrm{v}}_{i+\frac{1}{2},j} - \hat{F}^{\mathrm{v}}_{i-\frac{1}{2},j}\right) + \frac{1}{\Delta y}\left(\hat{G}^{\mathrm{v}}_{i,j+\frac{1}{2}} - \hat{G}^{\mathrm{v}}_{i,j-\frac{1}{2}}\right) + S_{i,j}(t), \end{aligned} \tag{2.2}$$

where

$$\begin{aligned} U_{i,j}(t) &\approx \frac{1}{\Delta x \Delta y} \int_{y_{j-\frac{1}{2}}}^{y_{j+\frac{1}{2}}} \int_{x_{i-\frac{1}{2}}}^{x_{i+\frac{1}{2}}} u(x, y, t)\mathrm{d}x\mathrm{d}y, \\ S_{i,j}(t) &\approx \frac{1}{\Delta x \Delta y} \int_{y_{j-\frac{1}{2}}}^{y_{j+\frac{1}{2}}} \int_{x_{i-\frac{1}{2}}}^{x_{i+\frac{1}{2}}} s(u, x, y, t)\mathrm{d}x\mathrm{d}y \end{aligned}$$

are the numerical approximations of the exact cell averages of the conserved quantity and source term, and

$$
\begin{aligned}
\hat{F}_{i+\frac{1}{2},j} &\approx \bar{f}_{i+\frac{1}{2},j} \equiv \frac{1}{\Delta y}\int_{y_{j-\frac{1}{2}}}^{y_{j+\frac{1}{2}}} f(u(x_{i+\frac{1}{2}},y,t))\mathrm{d}y,\\
\hat{G}_{i,j+\frac{1}{2}} &\approx \bar{g}_{i,j+\frac{1}{2}} \equiv \frac{1}{\Delta x}\int_{x_{i-\frac{1}{2}}}^{x_{i+\frac{1}{2}}} g(u(x,y_{j+\frac{1}{2}},t))\mathrm{d}x,\\
\hat{F}^{\mathrm{v}}_{i+\frac{1}{2},j} &\approx \overline{f^{\mathrm{v}}}_{i+\frac{1}{2},j} \equiv \frac{1}{\Delta y}\int_{y_{j-\frac{1}{2}}}^{y_{j+\frac{1}{2}}} f^{\mathrm{v}}(u,\nabla u)|_{x_{i+\frac{1}{2}}}\mathrm{d}y,\\
\hat{G}^{\mathrm{v}}_{i,j+\frac{1}{2}} &\approx \overline{g^{\mathrm{v}}}_{i,j+\frac{1}{2}} \equiv \frac{1}{\Delta x}\int_{x_{i-\frac{1}{2}}}^{x_{i+\frac{1}{2}}} g^{\mathrm{v}}(u,\nabla u)|_{y_{j+\frac{1}{2}}}\mathrm{d}x
\end{aligned}
$$

are the numerical approximations of the exact edge averages of the convective and viscous fluxes.

In the dimension-by-dimension FV WENO method, 1D WENO reconstructions from known cell-averaged conserved quantities $\{U_{i,j}\}$ are made for the convective terms. Similarly, for the diffusion terms, we construct $(p-1)$-th degree polynomials $q^1(x)$ in the x direction and $q^2(y)$ in the y direction by 1D sixth-order accurate central reconstruction (CR6) (Vevek et al. 2019) for the conserved quantity, which represent local approximations of the conserved quantity at cell interfaces averaged in another coordinate. They are constructed by satisfying

$$
U_{m,j} = \frac{1}{\Delta x}\int_{x_{m-\frac{1}{2}}}^{x_{m+\frac{1}{2}}} \left[q^1(x)+\mathcal{O}(\Delta x^p)\right]\mathrm{d}x,\quad m\in[i-2,\ldots,i+3], \tag{2.3a}
$$

$$
U_{i,n} = \frac{1}{\Delta y}\int_{y_{n-\frac{1}{2}}}^{y_{n+\frac{1}{2}}} \left[q^2(y)+\mathcal{O}(\Delta y^p)\right]\mathrm{d}y,\quad n\in[j-2,\ldots,j+3] \tag{2.3b}
$$

with $p=6$ in this paper. Note that the stencil of CR6 (six cells from $i-2$ to $i+3$ in Fig. 1) for reconstructing $U_{i+\frac{1}{2},j}$ is symmetrical with respect to the interface $x_{i+1/2}$ to provide the necessary isotropic diffusion.

If $U_{m,j}$ are exact cell averages of the conserved quantity, then Eq. (2.3a) indicates that

$$
q^1(x) = \frac{1}{\Delta y}\int_{y_{j-\frac{1}{2}}}^{y_{j+\frac{1}{2}}} u(x,y)\mathrm{d}y + \mathcal{O}(\Delta x^p), \tag{2.4}
$$

and it can be seen easily that the derivative and integration are interchangeable:

$$
\partial_x q^1(x) = \frac{1}{\Delta y}\int_{y_{j-\frac{1}{2}}}^{y_{j+\frac{1}{2}}} \partial_x u(x,y)\mathrm{d}y + \mathcal{O}(\Delta x^{p-1}). \tag{2.5}
$$

Similar results hold for $q^2(y)$ in the y direction.

By evaluating the polynomials and their derivatives at interfaces, we get the reconstructed edge-averaged values of the conserved quantity and its derivative at the cell interface as

$$
\begin{aligned}
U_{i+\frac{1}{2},j} &:= q^1\left(x_{i+\frac{1}{2},j}\right),\quad U_{i,j+\frac{1}{2}} := q^2\left(y_{i,j+\frac{1}{2}}\right).\\
\partial_x U_{i+\frac{1}{2},j} &:= \partial_x q^1\left(x_{i+\frac{1}{2},j}\right),\quad \partial_y U_{i,j+\frac{1}{2}} := \partial_y q^2\left(y_{i,j+\frac{1}{2}}\right).
\end{aligned} \tag{2.6}
$$

The corresponding exact edge-averaged values of the conserved quantity and its derivative at the cell interface are denoted by

$$\begin{aligned}\overline{u}_{i+\frac{1}{2},j} &:= \frac{1}{\Delta y}\int_{y_{j-\frac{1}{2}}}^{y_{j+\frac{1}{2}}} u(x_{i+\frac{1}{2}},y)\mathrm{d}y, \quad \overline{u}_{i,j+\frac{1}{2}} := \frac{1}{\Delta x}\int_{x_{i-\frac{1}{2}}}^{x_{i+\frac{1}{2}}} u(x,y_{j+\frac{1}{2}})\mathrm{d}x,\\ \overline{\partial_x u}_{i+\frac{1}{2},j} &:= \frac{1}{\Delta y}\int_{y_{j-\frac{1}{2}}}^{y_{j+\frac{1}{2}}} \partial_x u(x_{i+\frac{1}{2}},y)\mathrm{d}y, \quad \overline{\partial_y u}_{i,j+\frac{1}{2}} := \frac{1}{\Delta x}\int_{x_{i-\frac{1}{2}}}^{x_{i+\frac{1}{2}}} \partial_y u(x,y_{j+\frac{1}{2}})\mathrm{d}x.\end{aligned} \tag{2.7}$$

From Eqs. (2.4) and (2.5), we see that the reconstructed edge-averaged values satisfy

$$\begin{aligned}U_{i+\frac{1}{2},j} &= \overline{u}_{i+\frac{1}{2},j} + \mathcal{O}(\Delta x^p), \quad U_{i,j+\frac{1}{2}} = \overline{u}_{i,j+\frac{1}{2}} + \mathcal{O}(\Delta y^p),\\ \partial_x U_{i+\frac{1}{2},j} &= \overline{\partial_x u}_{i+\frac{1}{2},j} + \mathcal{O}(\Delta x^{p-1}), \quad \partial_y U_{i,j+\frac{1}{2}} = \overline{\partial_y u}_{i,j+\frac{1}{2}} + \mathcal{O}(\Delta y^{p-1}),\end{aligned} \tag{2.8}$$

In the dimension-by-dimension approach, the numerical viscous flux in Eq. (2.2) is computed by $\hat{F}^{\mathrm{v}}_{i+1/2,j} = f^{\mathrm{v}}(U_{i+1/2,j}, \partial_x U_{i+1/2,j}, \partial_y U_{i+1/2,j})$. We assume that the viscous flux function f^{v} is Lipschitz continuous. For variable diffusion coefficient cases, this numerical viscous flux $\hat{F}^{\mathrm{v}}_{i+1/2,j}$ generally leads to only second-order accuracy. It should be noted that the third argument (the cross derivative $\partial_y U_{i+1/2,j}$ in f^{v}) does not affect the following second-order accuracy conclusion; thus, it is omitted in the following analysis. The accuracy analysis proceeds as follows. By the Lipschitz continuity, we have

$$\begin{aligned}|\hat{F}^{\mathrm{v}}_{i+\frac{1}{2},j} - f^{\mathrm{v}}(\overline{u}_{i+\frac{1}{2},j}, \overline{\partial_x u}_{i+\frac{1}{2},j})| &= |f^{\mathrm{v}}(U_{i+\frac{1}{2},j}, \partial_x U_{i+\frac{1}{2},j}) - f^{\mathrm{v}}(\overline{u}_{i+\frac{1}{2},j}, \overline{\partial_x u}_{i+\frac{1}{2},j})|\\ &\le |f^{\mathrm{v}}(U_{i+\frac{1}{2},j}, \partial_x U_{i+\frac{1}{2},j}) - f^{\mathrm{v}}(U_{i+\frac{1}{2},j}, \overline{\partial_x u}_{i+\frac{1}{2},j})|\\ &\quad + |f^{\mathrm{v}}(U_{i+\frac{1}{2},j}, \overline{\partial_x u}_{i+\frac{1}{2},j}) - f^{\mathrm{v}}(\overline{u}_{i+\frac{1}{2},j}, \overline{\partial_x u}_{i+\frac{1}{2},j})|\\ &\le L\left(|U_{i+\frac{1}{2},j} - \overline{u}_{i+\frac{1}{2},j}| + |\partial_x U_{i+\frac{1}{2},j} - \overline{\partial_x u}_{i+\frac{1}{2},j}|\right)\\ &= \mathcal{O}(\Delta x^p) + \mathcal{O}(\Delta x^{p-1})\\ &= \mathcal{O}(\Delta x^{p-1}).\end{aligned}$$

That is,

$$\hat{F}^{\mathrm{v}}_{i+\frac{1}{2},j} = f^{\mathrm{v}}\left(\overline{u}_{i+\frac{1}{2},j}, \overline{\partial_x u}_{i+\frac{1}{2},j}\right) + \mathcal{O}(\Delta x^{p-1}). \tag{2.9}$$

Assuming that the leading term in the error $\mathcal{O}(\Delta x^{p-1})$ is smooth, we have

$$\frac{\hat{F}^{\mathrm{v}}_{i+\frac{1}{2},j} - \hat{F}^{\mathrm{v}}_{i-\frac{1}{2},j}}{\Delta x} = \frac{f^{\mathrm{v}}\left(\overline{u}_{i+\frac{1}{2},j}, \overline{\partial_x u}_{i+\frac{1}{2},j}\right) - f^{\mathrm{v}}\left(\overline{u}_{i-\frac{1}{2},j}, \overline{\partial_x u}_{i-\frac{1}{2},j}\right)}{\Delta x} + \mathcal{O}(\Delta x^{p-1}). \tag{2.10}$$

From Eq. (2.7) and noting that the edge-averaged value of any space-dependent function generally agrees with the point value at the edge center point to second order, we have

$$\begin{aligned}\overline{u}_{i+\frac{1}{2},j} &= u_{i+\frac{1}{2},j} + \frac{u_{yy}(x_{i+\frac{1}{2}},\xi)}{24}\Delta y^2 + \mathcal{O}\left(\Delta y^4\right), \quad \xi \in (y_{j-\frac{1}{2}}, y_{j+\frac{1}{2}}),\\ \overline{\partial_x u}_{i+\frac{1}{2},j} &= \partial_x u_{i+\frac{1}{2},j} + \frac{u_{xyy}(x_{i+\frac{1}{2}},\xi)}{24}\Delta y^2 + \mathcal{O}\left(\Delta y^4\right), \quad \xi \in (y_{j-\frac{1}{2}}, y_{j+\frac{1}{2}}),\end{aligned} \tag{2.11}$$

and similarly,

$$\overline{f^{\mathrm{v}}}_{i+\frac{1}{2},j} = f^{\mathrm{v}}_{i+\frac{1}{2},j} + \frac{f^{\mathrm{v}}_{yy}\left(u(x_{i+\frac{1}{2}},\xi),\partial_x u(x_{i+\frac{1}{2}},\xi)\right)}{24}\Delta y^2 \\ +\mathcal{O}\left(\Delta y^4\right),\quad \xi\in(y_{j-\frac{1}{2}},y_{j+\frac{1}{2}}). \tag{2.12}$$

The function f^{v} can be expanded using Taylor series expansion, and the use of (2.11) gives

$$f^{\mathrm{v}}\left(\overline{u}_{i+\frac{1}{2},j},\ \overline{\partial_x u}_{i+\frac{1}{2},j}\right) = f^{\mathrm{v}}_{i+\frac{1}{2},j} + \frac{f^{\mathrm{v}}_u|_{(x_{i+\frac{1}{2}},y_j)}u_{yy}(x_{i+\frac{1}{2}},\xi) + f^{\mathrm{v}}_{\partial_x u}|_{(x_{i+\frac{1}{2}},y_j)}u_{xyy}(x_{i+\frac{1}{2}},\xi)}{24}\Delta y^2 \\ +\mathcal{O}\left(\Delta y^4\right). \tag{2.13}$$

From Eqs. (2.13), (2.12) and (2.9), we have

$$\begin{aligned}\overline{f^{\mathrm{v}}}_{i+\frac{1}{2},j} &= f^{\mathrm{v}}\left(\overline{u}_{i+\frac{1}{2},j},\ \overline{\partial_x u}_{i+\frac{1}{2},j}\right) + \mathcal{O}\left(\Delta y^2\right)\\ &= \hat{F}^{\mathrm{v}}_{i+\frac{1}{2},j} + \mathcal{O}\left(\Delta y^2\right) + \mathcal{O}\left(\Delta x^{p-1}\right),\end{aligned} \tag{2.14}$$

which is the crucial source of second-order error regardless of the order of reconstruction. Assuming that the leading term in the error $\mathcal{O}(\Delta y^2)$ is smooth, we have

$$\begin{aligned}&\frac{\overline{f^{\mathrm{v}}}_{i+\frac{1}{2},j} - \overline{f^{\mathrm{v}}}_{i-\frac{1}{2},j}}{\Delta x} - \frac{\hat{F}^{\mathrm{v}}_{i+\frac{1}{2},j} - \hat{F}^{\mathrm{v}}_{i-\frac{1}{2},j}}{\Delta x}\\ &= \frac{\overline{f^{\mathrm{v}}}_{i+\frac{1}{2},j} - \overline{f^{\mathrm{v}}}_{i-\frac{1}{2},j}}{\Delta x} - \frac{f^{\mathrm{v}}(\overline{u}_{i+\frac{1}{2},j},\overline{\partial_x u}_{i+\frac{1}{2},j}) - f^{\mathrm{v}}(\overline{u}_{i-\frac{1}{2},j},\overline{\partial_x u}_{i-\frac{1}{2},j})}{\Delta x} + \mathcal{O}(\Delta x^{p-1})\\ &= \frac{\overline{f^{\mathrm{v}}}_{i+\frac{1}{2},j} - f^{\mathrm{v}}(\overline{u}_{i+\frac{1}{2},j},\overline{\partial_x u}_{i+\frac{1}{2},j})}{\Delta x} - \frac{\overline{f^{\mathrm{v}}}_{i-\frac{1}{2},j} - f^{\mathrm{v}}(\overline{u}_{i-\frac{1}{2},j},\overline{\partial_x u}_{i-\frac{1}{2},j})}{\Delta x} + \mathcal{O}(\Delta x^{p-1})\\ &= \mathcal{O}(\Delta y^2 + \Delta x^{p-1}).\end{aligned} \tag{2.15}$$

Similar result holds for $\hat{G}^{\mathrm{v}}$ in the y-direction.

Thus, the dimension-by-dimension FV method for the diffusion terms with space-dependent diffusion coefficients is generally only second-order accurate in space. But in the "linear" case, i.e., if $f^{\mathrm{v}}(u,u_x,u_y) = Au_x + Bu_y$ with constant matrices $A, B \in \mathbb{R}^{m\times m}$, then

$$\int_{y_{j-\frac{1}{2}}}^{y_{j+\frac{1}{2}}} f^{\mathrm{v}}(u,u_x,u_y)\big|_{x_{i+\frac{1}{2}}}\,\mathrm{d}y = A\int_{y_{j-\frac{1}{2}}}^{y_{j+\frac{1}{2}}}\partial_x u(x_{i+\frac{1}{2}},y)\mathrm{d}y + B\int_{y_{j-\frac{1}{2}}}^{y_{j+\frac{1}{2}}}\partial_y u\left(x_{i+\frac{1}{2}},y\right)\mathrm{d}y,$$

that is, instead of (2.14), we now have

$$\overline{f^{\mathrm{v}}}_{i+\frac{1}{2},j} = A\overline{\partial_x u}_{i+\frac{1}{2},j} + B\overline{\partial_y u}_{i+\frac{1}{2},j}, \tag{2.16}$$

therefore, avoiding the crucial second-order error $\mathcal{O}(\Delta y^2)$. From (2.15), we can get

$$\frac{\overline{f^{\mathrm{v}}}_{i+\frac{1}{2},j} - \overline{f^{\mathrm{v}}}_{i-\frac{1}{2},j}}{\Delta x} - \frac{\hat{F}^{\mathrm{v}}_{i+\frac{1}{2},j} - \hat{F}^{\mathrm{v}}_{i-\frac{1}{2},j}}{\Delta x} = \mathcal{O}(\Delta x^{p-1}), \tag{2.17}$$

which leads to $(p-1)$th order in the local truncation error for this linear case.

3 Modified finite-volume method

3.1 Conversion between average values and point values

To improve the accuracy of the classical dimension-by-dimension FV method, we adopt high-order conversions between edge-averaged values and edge center point values of any sufficiently smooth function (Buchmüller and Helzel 2014). We first compute fourth-order accurate point values of the conserved quantity and their normal derivatives at the center of the grid cell interface from reconstructed edge-averaged values using the conversion formulas (Buchmüller and Helzel 2014; Buchmüller et al. 2016, 2018) for Eqs. (2.7) and (2.8), which gives

$$\begin{aligned} u\left(x_{i+\frac{1}{2}}, y_j\right) &= \bar{u}_{i+\frac{1}{2},j} - \frac{\Delta y^2}{24} u_{yy}\left(x_{i+\frac{1}{2}}, y_j\right) - \frac{\Delta y^4}{1920} u_{yyyy}\left(x_{i+\frac{1}{2}}, y_j\right) + \cdots \\ &= U_{i+\frac{1}{2},j} - \frac{\Delta y^2}{24} u_{yy}\left(x_{i+\frac{1}{2}}, y_j\right) - \frac{\Delta y^4}{1920} u_{yyyy}\left(x_{i+\frac{1}{2}}, y_j\right) + \cdots + \mathcal{O}\left(\Delta x^p\right), \\ \partial_x u\left(x_{i+\frac{1}{2}}, y_j\right) &= \overline{\partial_x u}_{i+\frac{1}{2},j} - \frac{\Delta y^2}{24} (u_x)_{yy}\left(x_{i+\frac{1}{2}}, y_j\right) - \frac{\Delta y^4}{1920} (u_x)_{yyyy}\left(x_{i+\frac{1}{2}}, y_j\right) + \cdots \\ &= \partial_x U_{i+\frac{1}{2},j} - \frac{\Delta y^2}{24} (u_x)_{yy}\left(x_{i+\frac{1}{2}}, y_j\right) - \frac{\Delta y^4}{1920} (u_x)_{yyyy}\left(x_{i+\frac{1}{2}}, y_j\right) \\ &\quad + \cdots + \mathcal{O}(\Delta x^{p-1}). \end{aligned} \tag{3.1}$$

Analogous formulas exist for edge center values and edge-averaged values of the conserved quantity and its normal derivative at the grid cell interface in the y-direction.

To achieve fourth-order accuracy, we need to approximate the derivatives u_{yy} and $(u_x)_{yy}$ in the second terms of the RHS of Eq. (3.1) with second-order accuracy. Thanks to the observation (Tamaki and Imamura 2017) that the differentiation and the averaging operation are exchangeable, e.g., $\bar{u}_{yy} = \overline{u_{yy}}$. We can simply get a conversion formula similar to (3.1)

$$\begin{aligned} u_{yy}(x_{i+1/2}, y_j) &= (\overline{u_{yy}})_{i+1/2,j} - \frac{\Delta y^2}{24} u_{yyyy}(x_{i+\frac{1}{2}}, y_j) + \mathcal{O}(\Delta y^4) \\ &= (\bar{u}_{yy})_{i+1/2,j} + \mathcal{O}(\Delta y^2) \\ &= (U_{yy})_{i+1/2,j} + \mathcal{O}(\Delta y^2) + \mathcal{O}(\Delta x^p). \end{aligned} \tag{3.2}$$

Thus, the first equality of (3.1) becomes

$$\begin{aligned} u(x_{i+\frac{1}{2}}, y_j) &= U_{i+\frac{1}{2},j} - \frac{\Delta y^2}{24}\left((U_{yy})_{i+\frac{1}{2},j} + \mathcal{O}(\Delta y^2) + \mathcal{O}(\Delta x^p)\right) + \mathcal{O}(\Delta y^4) + \mathcal{O}(\Delta x^p) \\ &= U_{i+\frac{1}{2},j} - \frac{1}{24}\left(U_{i+\frac{1}{2},j-1} - 2U_{i+\frac{1}{2},j} + U_{i+\frac{1}{2},j+1}\right) + \mathcal{O}(\Delta y^4) + \mathcal{O}(\Delta x^p). \end{aligned} \tag{3.3}$$

The same procedure can be applied to the normal derivative u_x, so that the second equality of (3.1) becomes

$$\begin{aligned} \partial_x u(x_{i+\frac{1}{2}}, y_j) = \partial_x U_{i+\frac{1}{2},j} &- \frac{1}{24}\left(\partial_x U_{i+\frac{1}{2},j-1} - 2\partial_x U_{i+\frac{1}{2},j} + \partial_x U_{i+\frac{1}{2},j+1}\right) \\ &+ \mathcal{O}(\Delta y^4) + \mathcal{O}(\Delta x^{p-1}). \end{aligned} \tag{3.4}$$

To computer point values of the cross derivative $\partial_y u_{i+1/2,j}$ at the center of the grid cell interface as needed by the viscous flux $f^{\mathrm{v}}_{i+1/2,j}$, we use point values of the conserved quantity

$u_{i+1/2,j}$ which have been obtained by Eq. (3.3) to approximate this cross derivative by a standard fourth-order accurate finite difference formula as the following:

$$\partial_y u_{i+\frac{1}{2},j} = \frac{8\left(u_{i+\frac{1}{2},j+1} - u_{i+\frac{1}{2},j-1}\right) - \left(u_{i+\frac{1}{2},j+2} - u_{i+\frac{1}{2},j-2}\right)}{12\Delta y} + \mathcal{O}(\Delta y^4). \quad (3.5)$$

Now the approximated point values, still denoted as $u_{i+1/2,j}$, $\partial_x u_{i+1/2,j}$, and $\partial_y u_{i+1/2,j}$, are directly used to compute the edge center point value of numerical viscous flux $\hat{f}^{\mathrm{v}}_{i+1/2,j}$

$$\hat{f}^{\mathrm{v}}_{i+1/2,j} = f^{\mathrm{v}}\left(u_{i+\frac{1}{2},j}, \partial_x u_{i+\frac{1}{2},j}, \partial_y u_{i+\frac{1}{2},j}\right). \quad (3.6)$$

Analogous formulas similar to Eqs. (3.3)–(3.6) can be obtained in the y direction to get point value of the numerical viscous flux $\hat{g}^{\mathrm{v}}_{i,j+1/2}$.

Finally, by substituting these point values of numerical viscous fluxes into Eq. (3.1) which is also valid for sufficiently smooth viscous flux function, we can compute fourth-order accurate edge-averaged numerical viscous fluxes as

$$\begin{aligned}
\hat{F}^{\mathrm{v}}_{i+\frac{1}{2},j} &= \hat{f}^{\mathrm{v}}_{i+\frac{1}{2},j} + \frac{1}{24}\left(\hat{f}^{\mathrm{v}}_{i+\frac{1}{2},j-1} - 2\hat{f}^{\mathrm{v}}_{i+\frac{1}{2},j} + \hat{f}^{\mathrm{v}}_{i+\frac{1}{2},j+1}\right) \\
&= f^{\mathrm{v}}_{i+\frac{1}{2},j} + \frac{1}{24}\left(f^{\mathrm{v}}_{i+\frac{1}{2},j-1} - 2f^{\mathrm{v}}_{i+\frac{1}{2},j} + f^{\mathrm{v}}_{i+\frac{1}{2},j+1}\right) \\
&= \overline{f^{\mathrm{v}}}_{i+\frac{1}{2},j} + \mathcal{O}(\Delta y^4) + \mathcal{O}(\Delta x^{p-1}), \\
\hat{G}^{\mathrm{v}}_{i,j+\frac{1}{2}} &= \hat{g}^{\mathrm{v}}_{i,j+\frac{1}{2}} + \frac{1}{24}\left(\hat{g}^{\mathrm{v}}_{i-1,j+\frac{1}{2}} - 2\hat{g}^{\mathrm{v}}_{i,j+\frac{1}{2}} + \hat{g}^{\mathrm{v}}_{i+1,j+\frac{1}{2}}\right) \\
&= g^{\mathrm{v}}_{i,j+\frac{1}{2}} + \frac{1}{24}\left(g^{\mathrm{v}}_{i-1,j+\frac{1}{2}} - 2g^{\mathrm{v}}_{i,j+\frac{1}{2}} + g^{\mathrm{v}}_{i+1,j+\frac{1}{2}}\right) \\
&= \overline{g^{\mathrm{v}}}_{i,j+\frac{1}{2}} + \mathcal{O}(\Delta x^4) + \mathcal{O}(\Delta y^{p-1}).
\end{aligned} \quad (3.7)$$

Comparing Eqs. (3.7) and (2.14), we see that the present numerical viscous fluxes are fourth-order accurate in space, while the original ones (2.14) are second-order accurate. The key to enhance accuracy is to use the transformations (3.3) and (3.4) from edge-averaged values to edge center values, a high-order finite difference for point values of the cross derivative, (3.5), and the transformation (3.7) from point values to edge-averaged values.

Figure 1 shows the stencil for computing the edge center point values of $u_{i+1/2,j}$ using (3.3) , $\partial_x u_{i+1/2,j}$ using (3.4), and the cross derivative $\partial_y u_{i+1/2,j}$ using (3.5). The transformations (3.3) and (3.4) require three edge-averaged values of $U_{i+1/2,j}$ and $\partial_x U_{i+1/2,j}$ marked as three green edges on the $i + 1/2$ line, each of which is obtained using the 1D sixth-order central reconstruction in the i direction using cell averages from $i-2$ to $i+3$. The cross derivative at the edge center $\partial_y u_{i+1/2,j}$ computed by the standard fourth-order accurate finite difference formula (3.5) requires four nearby edge center point values ($u_{i+1/2,j\pm1}$, $u_{i+1/2,j\pm2}$).

Figure 2 shows the stencil for computing the edge-averaged value of the viscous flux $\hat{F}^{\mathrm{v}}_{i+1/2,j}$ marked as the red edge using the transformation (3.7). This requires three point values of fluxes $\hat{f}^{\mathrm{v}}_{i+1/2,j}$ marked as red points, and each point resides values of $u_{i+1/2,j}$, $\partial_x u_{i+1/2,j}$ and $\partial_y u_{i+1/2,j}$ that further involve seven i-direction central reconstructions as required by Eqs. (3.3), (3.4) and (3.5). All the shaded cells compose the stencil for computing the edge-averaged flux $\hat{F}^{\mathrm{v}}_{i+1/2,j}$.

We remark that similar transformations between edge-averaged values and point values are used to obtain fourth-order accurate numerical convective fluxes $\hat{F}_{i+1/2,j}$ and $\hat{G}_{i,j+1/2}$ for the FV method as done in Buchmüller and Helzel (2014). We will not repeat them here.

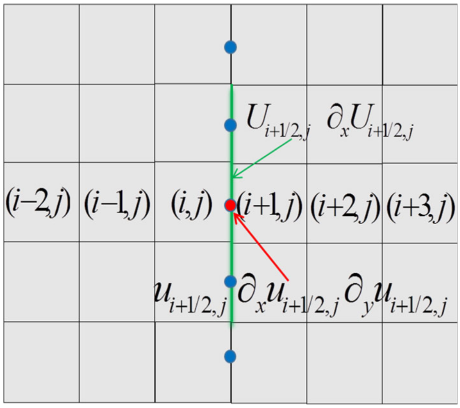

Fig. 1 The stencil for computing the edge center point values $u_{i+1/2,j}$, $\partial_x u_{i+1/2,j}$ and $\partial_y u_{i+1/2,j}$ marked as the red point. The three green edges denote edge-averaged values of $U_{i+1/2,j}$ and $\partial_x U_{i+1/2,j}$ obtained from 1D central reconstructions and required by Eqs. (3.3) and (3.4). Four nearby point values of $(u_{i+1/2,j\pm 1}, u_{i+1/2,j\pm 2})$ marked as the blue points are used to computed the point values of the cross derivative $\partial_y u_{i+1/2,j}$ by Eq. (3.5)

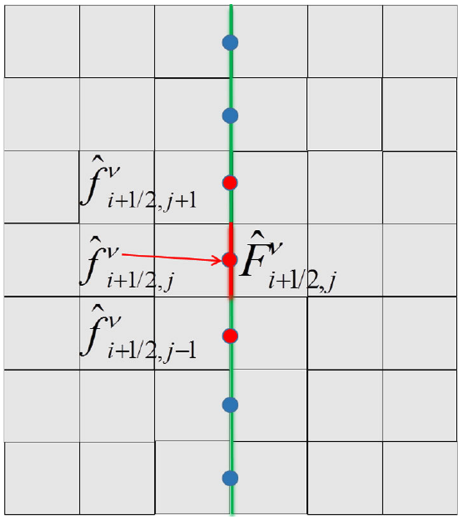

Fig. 2 The stencil for computing the edge averaged flux $\hat{F}^{\mathrm{v}}_{i+1/2,j}$ marked as red edge. Three red point viscous flux values of $\hat{f}^{\mathrm{v}}_{i+1/2,j}$ are required to compute $\hat{F}^{\mathrm{v}}_{i+1/2,j}$ by Eq. (3.7). The three red viscous flux points require point values of $u_{i+1/2,j}$, $\partial_x u_{i+1/2,j}$ and $\partial_y u_{i+1/2,j}$ residing at the red and blue points that further need seven reconstructed $U_{i+1/2,j}$ and $\partial_x U_{i+1/2,j}$ on the green line, which involve all the grey cells

3.2 Algorithm for modified FV method

When combined with the improved fifth-order WENO FV method for hyperbolic conservation laws (Buchmüller and Helzel 2014), the present conversion formulas (3.3)–(3.7) between point values and edge-averaged vales for the viscous fluxes suggest the following modified dimension-by-dimension FV method for convection–diffusion equations.

Algorithm: modified FV method for convection–diffusion equation

(1) Compute edge-averaged values of the conserved quantity and its spatial derivatives at cell interfaces using 1D WENO reconstructions for the convection terms and 1D central reconstructions (CR) for the diffusion terms, respectively, i.e., compute

$$U^{\pm}_{i+\frac{1}{2},j},\quad U^{\pm}_{i,j+\frac{1}{2}},\quad \text{and}\quad U_{i+\frac{1}{2},j},\quad \partial_x U_{i+\frac{1}{2},j},\quad U_{i,j+\frac{1}{2}},\quad \partial_y U_{i,j+\frac{1}{2}}$$

at all cell interfaces.

Table 1 Predicted convergence rate for different methods

Method	WENOZ5+CR6+RK5		
	Linear convection and diffusion terms	Nonlinear convection term	Varying coefficient diffusion term
Classical method	5	2	2
Modified method	4	4	4

(2) Compute point values of the conserved quantity and its derivatives at the center points of grid cell interfaces for the convective and viscous terms, respectively, i.e., compute

$$u^{\pm}_{i+\frac{1}{2},j},\quad u^{\pm}_{i,j+\frac{1}{2}},\quad \text{and}\quad u_{i+\frac{1}{2},j},\quad \partial_x u_{i+\frac{1}{2},j},\quad \partial_y u_{i+\frac{1}{2},j},$$
$$u_{i,j+\frac{1}{2}},\quad \partial_y u_{i,j+\frac{1}{2}},\quad \partial_x u_{i,j+\frac{1}{2}}$$

using the conversion formulas (3.3)–(3.5).

(3) Compute convective and viscous numerical fluxes at center points of the cell interfaces

$$\begin{aligned}
\hat{f}_{i+\frac{1}{2},j} &= \mathcal{F}\left(u^{-}_{i+\frac{1}{2},j}, u^{+}_{i+\frac{1}{2},j}\right), \quad \hat{g}_{i,j+\frac{1}{2}} = \mathcal{F}\left(u^{-}_{i,j+\frac{1}{2}}, u^{+}_{i,j+\frac{1}{2}}\right),\\
\hat{f}^{\mathrm{v}}_{i+\frac{1}{2},j} &= f^{\mathrm{v}}\left(u_{i+\frac{1}{2},j}, \partial_x u_{i+\frac{1}{2},j}, \partial_y u_{i+\frac{1}{2},j}\right),\\
\hat{g}^{\mathrm{v}}_{i,j+\frac{1}{2}} &= g^{\mathrm{v}}\left(u_{i,j+\frac{1}{2}}, \partial_x u_{i,j+\frac{1}{2}}, \partial_y u_{i,j+\frac{1}{2}}\right),
\end{aligned}$$

where $\mathcal{F}(u^-, u^+)$ is a numerical flux function which is either the Lax–Friedrichs or HLLC flux in this work, and $f^{\mathrm{v}}(u, \nabla u)$ and $g^{\mathrm{v}}(u, \nabla u)$ are the viscous flux functions defined in differential equations.

(4) Compute edge-averaged values of convective and viscous numerical fluxes at grid cell interfaces, i.e., compute

$$\hat{F}_{i+\frac{1}{2},j},\quad \hat{G}_{i,j+\frac{1}{2}}\quad \text{and}\quad \hat{F}^{\mathrm{v}}_{i+\frac{1}{2},j},\quad \hat{G}^{\mathrm{v}}_{i,j+\frac{1}{2}}$$

using the conversion formula (3.7).

(5) Solve the semi-discrete system (2.2), using a high-order accurate Runge–Kutta method.

In Table 1, we summarize the expected convergence rates of the standard dimension-by-dimension FV method and the modified FV method for the approximation of linear and nonlinear convection–diffusion equations. We use the fifth-order accurate WENO-Z reconstruction (WENOZ5) (Borges et al. 2008; Don and Borges 2013) with the parameters $q = 1$ and $\epsilon = 10^{-40}$ for the convection terms, and sixth-order accurate central reconstruction (CR6) (Vevek et al. 2019) for $U_{i+1/2,j}$ (the corresponding $\partial_x U_{i+1/2,j}$ is fifth-order accurate) for the diffusion terms. To match the order of spatial accuracy, a fifth-order explicit Runge–Kutta scheme (RK5) [see Appendix 1 in Buchmüller and Helzel (2014)] is used.

4 Numerical results

In this section, several 2D numerical examples are used to compare the performance of the present modified dimension-by-dimension FV method and the classic dimension-by-dimension FV method for convection–diffusion equations.

Table 2 Convergence study for problem (4.1) with WENOZ5, CR6 and RK5

Grid	Classical method				Modified method			
	$\|\bar{u}-\bar{u}_{\text{exact}}\|_1$	EOC	$\|\bar{u}-\bar{u}_{\text{exact}}\|_\infty$	EOC	$\|\bar{u}-\bar{u}_{\text{exact}}\|_1$	EOC	$\|\bar{u}-\bar{u}_{\text{exact}}\|_\infty$	EOC
10^2	1.359×10^{-3}		1.956×10^{-3}		1.361×10^{-3}		1.961×10^{-3}	
20^2	4.004×10^{-5}	5.09	6.169×10^{-5}	4.99	4.007×10^{-5}	5.08	6.267×10^{-5}	4.97
40^2	1.196×10^{-6}	5.07	1.879×10^{-6}	5.04	1.284×10^{-6}	4.96	2.009×10^{-6}	4.96
80^2	3.708×10^{-8}	5.01	5.826×10^{-8}	5.01	5.486×10^{-8}	4.55	8.611×10^{-8}	4.54
160^2	1.159×10^{-9}	5.00	1.820×10^{-9}	5.00	3.102×10^{-9}	4.14	4.872×10^{-9}	4.14

In the following tables to show convergence studies, the norms of errors $\|\cdot\|_1 = \sum_{i,j}|\bar{u}_{i,j}-\bar{u}_{i,j}^{\text{exact}}|\Delta x\Delta y$ and $\|\cdot\|_\infty = \max_{i,j}|\bar{u}_{i,j}-\bar{u}_{i,j}^{\text{exact}}|$ are considered for that $\|\cdot\|_1$ provides a global view of the errors in average and $\|\cdot\|_\infty$ gives an assessment of the very local errors, where $\bar{u}$ represents the numerical cell average. We compute the experimental order of convergence (EOC) using the formula

$$\text{EOC} = \frac{\log\left(\|\bar{u}_m-\bar{u}_{\text{exact}}\|/\|\bar{u}_{2m}-\bar{u}_{\text{exact}}\|\right)}{\log 2},$$

where the index m indicates the number of grid cells in the x or y direction.

4.1 Scalar convection–diffusion problems

Several scalar convection–diffusion equations are given to verify the theoretical convergence order of accuracy for the modified FV method as expected in Table 1. In this subsection, the time step Δt is defined by $\frac{\text{CFL}\Delta^2}{\lambda\Delta+\mu}$ (Chou and Shu 2007), where $\Delta = \min\{\Delta x, \Delta y\}$, λ is the maximum convection speed, μ is the maximum diffusion coefficient, and CFL number is taken to be 0.2. The Lax–Friedrichs flux for the convective terms is used.

4.1.1 Linear convection–diffusion equation

We consider the 2D linear convection–diffusion problem (Sun et al. 2006) given by

$$\begin{cases} u_t + u_x + u_y - \mu(u_{xx}+u_{yy}) = 0 \\ u(x,y,0) = \sin\pi\,(x+y) \end{cases}, \quad -1 \le x, y \le 1 \tag{4.1}$$

with periodic boundary conditions. The exact solution is $u(x,y,t) = \exp(-2\pi^2\mu t)\sin\pi(x+y-2t)$. The final time is $T = 0.5$ and the diffusion coefficient $\mu = 0.1$.

In Table 2, we show the $\|\cdot\|_1$ and $\|\cdot\|_\infty$ errors and orders of convergence for the problem (4.1) computed with the two FV methods. Because both the convection terms and diffusion terms are linear in (4.1), as expected in Table 1, the classical method converges with fifth-order accuracy, but the modified method has achieved a little higher than the theoretical fourth-order of accuracy on the fine grids mainly due to the interaction between the fourth-order conversion and the sixth-order 1D reconstruction.

Table 3 Convergence study for problem (4.2) with WENOZ5, CR6 and RK5

Grid	Classical method				Modified method			
	$\|\bar{u}-\bar{u}_{\text{exact}}\|_1$	EOC	$\|\bar{u}-\bar{u}_{\text{exact}}\|_\infty$	EOC	$\|\bar{u}-\bar{u}_{\text{exact}}\|_1$	EOC	$\|\bar{u}-\bar{u}_{\text{exact}}\|_\infty$	EOC
10^2	2.626×10^{-4}		1.007×10^{-3}		4.349×10^{-5}		1.952×10^{-4}	
20^2	5.876×10^{-5}	2.16	2.133×10^{-4}	2.24	3.298×10^{-6}	3.72	1.340×10^{-5}	3.87
40^2	1.397×10^{-5}	2.07	5.017×10^{-5}	2.09	2.280×10^{-7}	3.85	8.610×10^{-7}	3.96
80^2	3.388×10^{-6}	2.04	1.223×10^{-5}	2.04	1.491×10^{-8}	3.93	5.352×10^{-8}	4.01
160^2	8.325×10^{-7}	2.03	3.019×10^{-6}	2.02	9.515×10^{-10}	3.97	3.347×10^{-9}	4.00

4.1.2 Nonlinear convection–linear diffusion equation

We consider the 2D steady-state nonlinear convection–linear diffusion problem (Chou and Shu 2007) given by

$$uu_x + u_y - u_{xx} = 0, \quad 0 \le x, y \le 1. \tag{4.2}$$

This problem has the steady-state solution

$$u(x, y, \infty) = -4\tanh(y + 2x) - \frac{1}{2},$$

with the exact solution imposed on the boundaries. We start from the initial condition $u(x, y, 0) = u(x, 0, 0)$ and compute steady-state solution by a pseudo-time marching. The residual is defined as (Zhang and Shu 2007)

$$\text{Res} = \frac{\sum_{i,j=1} |R_{i,j}|}{M \times N},$$

where $R_{i,j}$ is the local residual defined as

$$R_{i,j} = \frac{\bar{u}_{i,j}^{n+1} - \bar{u}_{i,j}^{n}}{\Delta t},$$

and $M \times N$ is the total number of grid cells. When Res $< 10^{-14}$, the steady state is assumed to be obtained.

In Table 3, we show the errors and grid convergence rates for problem (4.2) using the two different methods. In this problem, the convection term is nonlinear and the diffusion term is linear. Thus, the convergence rate of the classical method is only second order as expected in Table 1. In comparison, the order of convergence of the modified method has nearly reached fourth as shown in Table 3.

4.1.3 Nonlinear diffusion equation

We consider the 2D nonlinear diffusion problem (Cui et al. 2016; Sun et al. 2006) given by

$$\begin{cases} u_t - (uu_x)_x - (uu_y)_y = s(x, y, t), \\ s(x, y, t) = -\exp(-t)\exp(x + y) - 4\exp(-2t)\exp(2(x + y)), \quad 0 \le x, y \le 1. \\ u(x, y, 0) = \exp(x + y), \end{cases} \tag{4.3}$$

Table 4 Convergence study for problem (4.3) with WENOZ5, CR6 and RK5

Grid	Classical method				Modified method			
	$\|\bar{u}-\bar{u}_{\text{exact}}\|_1$	EOC	$\|\bar{u}-\bar{u}_{\text{exact}}\|_\infty$	EOC	$\|\bar{u}-\bar{u}_{\text{exact}}\|_1$	EOC	$\|\bar{u}-\bar{u}_{\text{exact}}\|_\infty$	EOC
10^2	3.197×10^{-4}		5.791×10^{-4}		1.457×10^{-6}		2.639×10^{-6}	
20^2	6.859×10^{-5}	2.22	1.335×10^{-4}	2.12	7.794×10^{-8}	4.22	1.517×10^{-7}	4.12
40^2	1.580×10^{-5}	2.12	3.192×10^{-5}	2.06	4.485×10^{-9}	4.12	9.062×10^{-9}	4.07
80^2	3.785×10^{-6}	2.06	7.794×10^{-6}	2.03	2.684×10^{-10}	4.06	5.553×10^{-10}	4.03
160^2	9.259×10^{-7}	2.03	1.926×10^{-7}	2.02	1.634×10^{-11}	4.04	3.404×10^{-11}	4.02

Table 5 Convergence study for problem (4.4) with WENOZ5, CR6 and RK5

Grid	Classical method				Modified method			
	$\|\bar{u}-\bar{u}_{\text{exact}}\|_1$	EOC	$\|\bar{u}-\bar{u}_{\text{exact}}\|_\infty$	EOC	$\|\bar{u}-\bar{u}_{\text{exact}}\|_1$	EOC	$\|\bar{u}-\bar{u}_{\text{exact}}\|_\infty$	EOC
10^2	1.920×10^{-3}		5.673×10^{-3}		1.348×10^{-4}		3.345×10^{-4}	
20^2	5.060×10^{-4}	1.92	1.666×10^{-3}	1.77	8.068×10^{-6}	4.06	2.442×10^{-5}	3.78
40^2	1.290×10^{-4}	1.97	4.806×10^{-4}	1.80	5.008×10^{-7}	4.01	1.653×10^{-6}	3.88
80^2	3.251×10^{-5}	1.99	1.266×10^{-4}	1.93	3.131×10^{-8}	4.00	1.060×10^{-7}	3.96
160^2	8.158×10^{-6}	1.99	3.212×10^{-5}	1.98	1.958×10^{-9}	4.00	6.753×10^{-9}	3.97

Dirichlet boundary conditions are implemented based on the exact solution $u(x, y, t) = \exp(-t)\exp(x + y)$. The final time is $T = 0.5$.

In Table 4, we show the errors and grid convergence rates for problem (4.3) obtained by the two different methods. Equation (4.3) has only nonlinear diffusion terms. One can observe that the computed EOCs agree with the expectations in Table 1. The convergence rate for the classical method is second order, while that for the modified method attains fourth order as shown in Table 4.

4.1.4 Linear diffusion equation with space-dependent coefficients

We consider the 2D linear diffusion problem with space-dependent coefficients (Xie and Zhang 2018) given by

$$\begin{cases} u_t - [(x+y)u_x]_x - \left[(x+y)u_y\right]_y = s(x,y,t), \\ s(x,y,t) = -\exp(-2t)\left[2(x+y-1)\sin(x+y) - 2\cos(x+y)\right], \quad 0 \le x, y \le 2\pi, \\ u(x,y,0) = \sin(x+y), \end{cases} \tag{4.4}$$

with periodic boundary conditions. The exact solution is $u(x, y, t) = \exp(-2t)\sin(x + y)$. The final time is $T = 0.5$.

We remark that while the pure space-dependent coefficients can lead to loss of accuracy in the classic dimension-by-dimension FV method, they can be easily evaluated at edge center points and used in the conversion (3.7) from edge center values to edge averaged vales for the viscous fluxes.

In Table 5, we show the errors and grid convergence rates for problem (4.4) calculated with the two different methods. Note that the diffusion terms are linear, however, they are with

Table 6 Convergence study for problem (4.5) with WENOZ5, CR6 and RK5

Grid	Classical method				Modified method			
	$\|\bar{u}-\bar{u}_{\text{exact}}\|_1$	EOC	$\|\bar{u}-\bar{u}_{\text{exact}}\|_\infty$	EOC	$\|\bar{u}-\bar{u}_{\text{exact}}\|_1$	EOC	$\|\bar{u}-\bar{u}_{\text{exact}}\|_\infty$	EOC
10^2	3.226×10^{-3}		9.202×10^{-3}		1.735×10^{-4}		5.365×10^{-4}	
20^2	8.508×10^{-4}	1.92	2.487×10^{-3}	1.89	1.179×10^{-5}	3.88	3.786×10^{-5}	3.82
40^2	2.152×10^{-4}	1.98	6.344×10^{-4}	1.97	7.469×10^{-7}	3.98	2.428×10^{-6}	3.96
80^2	5.397×10^{-5}	2.00	1.592×10^{-4}	1.99	4.680×10^{-8}	4.00	1.546×10^{-7}	3.97
160^2	1.350×10^{-5}	2.00	3.981×10^{-5}	2.01	2.927×10^{-9}	4.00	9.751×10^{-9}	3.99

space-dependent diffusion coefficient in Eq. (4.4). As expected in Table 1, the convergence rate for the classical method is second order and that for the modified method is fourth order as shown in Table 5.

4.1.5 Nonlinear convection–diffusion equation

We consider the 2D nonlinear convection–diffusion problem (Sun et al. 2006; Cui et al. 2016) given by

$$
\begin{cases}
u_t + uu_x + uu_y - [(1+xy+u)u_x]_x - \left[(1+xy+u)u_y\right]_y = s(x,y,t), \\
s(x,y,t) = -\exp(-t)\sin(\pi x)\sin(\pi y) + 2\pi^2\exp(-t)(1+xy)\sin(\pi x)\sin(\pi y) \\
\qquad -\pi y\exp(-t)\cos(\pi x)\sin(\pi y) - \pi x\exp(-t)\sin(\pi x)\cos(\pi y) \qquad\qquad 0\le x,y\le 2 \\
\qquad -\pi^2\exp(-2t)\left[\cos(2\pi x)\sin^2(\pi y)+\sin^2(\pi x)\cos(2\pi y)\right] \\
\qquad +\frac{\pi}{2}\exp(-2t)\left[\sin(2\pi x)\sin^2(\pi y)+\sin^2(\pi x)\sin(2\pi y)\right], \\
u(x,y,0) = \sin(\pi x)\sin(\pi y),
\end{cases}
\tag{4.5}
$$

with periodic boundary conditions. The exact solution is $u(x,y,t) = \exp(-t)\sin(\pi x)\sin(\pi y)$. The final time is $T = 0.5$.

In Table 6, we show the errors and grid convergence rates for problem (4.5) using the two different methods. In Eq. (4.5), both the convection terms and the diffusion terms are nonlinear. Thus, as expected in Table 1, the convergence rates for the classical method and the modified method are second and fourth order separately. The results in Table 6 confirm the above prediction.

4.2 2D Navier–Stokes equations

In this subsection, we consider the 2D compressible Navier–Stokes equations

$$
U_t + \nabla\cdot\mathbf{F}(U) = \nabla\cdot\mathbf{F}^{\text{v}}(U,\nabla U) + S, \tag{4.6}
$$

with the vector of the conservative variables U, the inviscid fluxes $\mathbf{F} = \left(F_1,\ F_2\right)^T$ and the viscous fluxes $\mathbf{F}^{\text{v}} = \left(F_1^{\text{v}},\ F_2^{\text{v}}\right)^T$ are given by

$$U = \begin{pmatrix} \rho \\ \rho v_1 \\ \rho v_2 \\ \rho E \end{pmatrix}, \quad F_\ell(U) = \begin{pmatrix} \rho v_\ell \\ \rho v_1 v_\ell + \delta_{1\ell} p \\ \rho v_2 v_\ell + \delta_{2\ell} p \\ v_\ell(\rho E + p) \end{pmatrix}, \quad F_\ell^{\mathrm{v}}(U, \nabla U) = \begin{pmatrix} 0 \\ \tau_{1\ell} \\ \tau_{2\ell} \\ \tau_{\ell 1} v_1 + \tau_{\ell 2} v_2 - q_\ell \end{pmatrix}, \tag{4.7}$$

with $\ell = 1, 2$. The viscous stress tensor is given by

$$\boldsymbol{\varnothing} = \mu \left(\nabla \mathbf{v} + (\nabla \mathbf{v})^T - \frac{2}{3} (\nabla \cdot \mathbf{v}) \mathbf{I} \right), \tag{4.8}$$

where $\mathbf{I}$ is the identity matrix, and the heat flux is by $\mathbf{q} = (q_1,\, q_2)^T$ with

$$q_1 = -k \frac{\partial T}{\partial x}, \;\; q_2 = -k \frac{\partial T}{\partial y}, \quad \text{with} \;\; k = \frac{\mu c_p}{Pr}. \tag{4.9}$$

In this paper, the dynamic viscosity μ, the Prandtl number Pr, the ratio of specific heats $\gamma = \frac{c_p}{c_v}$ with the specific heats c_p and c_v are all supposed to be constant. The system is closed with the equation of state of perfect gas

$$p = \rho R T = (\gamma - 1)\rho \left(E - \frac{1}{2} \mathbf{v} \cdot \mathbf{v} \right), \quad \text{and} \quad E = \frac{1}{2} \mathbf{v} \cdot \mathbf{v} + c_v T, \tag{4.10}$$

with the specific gas constant $R = c_p - c_v$. And the viscous fluxes are rewritten in the form

$$\mathbf{F}^{\mathrm{v}}(U, \nabla U) = \mathbf{D} \nabla U = \left(D_{11} U_x + D_{12} U_y,\; D_{21} U_x + D_{22} U_y \right), \tag{4.11}$$

where the solution-dependent matrix $\mathbf{D}$ is given by (Gassner et al. 2008; Yue et al. 2017)

$$\begin{aligned} \mathbf{D} &= \begin{pmatrix} D_{11} & D_{12} \\ D_{21} & D_{22} \end{pmatrix} \quad \text{with} \\ D_{11} &= \frac{\mu}{\rho} \begin{pmatrix} 0 & 0 & 0 & 0 \\ -\frac{4}{3} v_1 & \frac{4}{3} & 0 & 0 \\ -v_2 & 0 & 1 & 0 \\ \left(\frac{4}{3} v_1^2 + v_2^2 + \frac{\gamma}{Pr}(E - \mathbf{v}^2)\right) & (\frac{4}{3} - \frac{\gamma}{Pr}) v_1 & (1 - \frac{\gamma}{Pr}) v_2 & \frac{\gamma}{Pr} \end{pmatrix}, \\ D_{12} &= \frac{\mu}{\rho} \begin{pmatrix} 0 & 0 & 0 & 0 \\ \frac{2}{3} v_2 & 0 & -\frac{2}{3} & 0 \\ -v_1 & 1 & 0 & 0 \\ -\frac{1}{3} v_1 v_2 & v_2 & -\frac{2}{3} v_1 & 0 \end{pmatrix}, \quad D_{21} = \frac{\mu}{\rho} \begin{pmatrix} 0 & 0 & 0 & 0 \\ -v_2 & 0 & 1 & 0 \\ \frac{2}{3} v_1 & -\frac{2}{3} & 0 & 0 \\ -\frac{1}{3} v_1 v_2 & -\frac{2}{3} v_2 & v_1 & 0 \end{pmatrix}, \\ D_{22} &= \frac{\mu}{\rho} \begin{pmatrix} 0 & 0 & 0 & 0 \\ -v_1 & 1 & 0 & 0 \\ -\frac{4}{3} v_2 & 0 & \frac{4}{3} & 0 \\ -\left(v_1^2 + \frac{4}{3} v_2^2 + \frac{\gamma}{Pr}(E - \mathbf{v}^2)\right) & (1 - \frac{\gamma}{Pr}) v_1 & (\frac{4}{3} - \frac{\gamma}{Pr}) v_2 & \frac{\gamma}{Pr} \end{pmatrix}, \end{aligned} \tag{4.12}$$

which indicates that the viscous fluxes $\mathbf{F}^{\mathrm{v}}(U, \nabla U)$ are nonlinear about U.

For the numerical solution of the system (4.6) on Cartesian grids, the time step is evaluated from (Blazek 2005)

$$\Delta t = \frac{\mathrm{CFL} \cdot \Delta x \Delta y}{\max\limits_{\forall i,j} \left[\lambda_{i,j}^x \Delta y + \lambda_{i,j}^y \Delta x + 2 \max\left(\frac{4}{3\rho_{i,j}}, \frac{\gamma}{\rho_{i,j}} \right) \frac{\mu}{Pr} \right]}, \tag{4.13}$$

Table 7 Convergence study for exact solution (4.14) of N–S equations (4.6) with WENOZ5, CR6 and RK5

Grid	Classical method				Modified method			
	$\Vert\bar{u}-\bar{u}_{\text{exact}}\Vert_1$	EOC	$\Vert\bar{u}-\bar{u}_{\text{exact}}\Vert_\infty$	EOC	$\Vert\bar{u}-\bar{u}_{\text{exact}}\Vert_1$	EOC	$\Vert\bar{u}-\bar{u}_{\text{exact}}\Vert_\infty$	EOC
10^2	2.553×10^{-3}		6.248×10^{-3}		3.427×10^{-3}		7.507×10^{-3}	
20^2	3.863×10^{-4}	2.72	7.024×10^{-4}	3.15	1.324×10^{-4}	4.69	2.604×10^{-4}	4.85
40^2	1.223×10^{-4}	1.66	2.111×10^{-4}	1.73	3.262×10^{-6}	5.34	6.607×10^{-6}	5.30
80^2	3.169×10^{-5}	1.95	5.414×10^{-5}	1.96	5.952×10^{-8}	5.78	1.370×10^{-7}	5.59
160^2	7.945×10^{-6}	2.00	1.358×10^{-5}	2.00	2.430×10^{-9}	4.61	6.187×10^{-9}	4.47

where $\lambda^x_{i,j}$ and $\lambda^y_{i,j}$ denote the maximum local eigenvalues of the inviscid Jacobian matrices in the x and y directions, respectively. CFL number is taken to be 0.5. The HLLC numerical flux for the convective terms is used in this section.

4.2.1 Smooth nonlinear problem

To investigate the experimental order of convergence of the proposed modified method, an inhomogeneous problem for the 2D Navier–Stokes equations with source terms is chosen (Gassner et al. 2008). The exact solution to Eq. (4.6) is chosen to be

$$U=\begin{pmatrix}\sin\left(2(x+y)-t\right)+4\\ \sin\left(2(x+y)-t\right)+4\\ \sin\left(2(x+y)-t\right)+4\\ \left(\sin\left(2(x+y)-t\right)+4\right)^2\end{pmatrix} \tag{4.14}$$

with the source terms given as follows:

$$S=\begin{pmatrix}3\cos\left(2(x+y)-t\right)\\ \cos\left(2(x+y)-t\right)(14\gamma-9)+\sin\left(4(x+y)-2t\right)(2\gamma-2)\\ \cos\left(2(x+y)-t\right)(14\gamma-9)+\sin\left(4(x+y)-2t\right)(2\gamma-2)\\ \cos\left(2(x+y)-t\right)(28\gamma-4)+\sin\left(4(x+y)-2t\right)(4\gamma-1)+\frac{8\mu\gamma}{Pr}\sin\left(2(x+y)-t\right)\end{pmatrix}. \tag{4.15}$$

Additionally, the computational domain is chosen to be $[0,\pi]^2$, $\gamma=1.4$, $Pr=0.72$ and $\mu=1.0$ with periodic boundary conditions. The final time is $T=0.5$.

Table 7 shows the errors and grid convergence rates of the two FV methods for computing the N–S equations (4.6) with the source term (4.15). It is known that the N–S equations (4.6) have nonlinear convection terms and nonlinear diffusion terms. Thus the classical dimension-by-dimension FV method has only second order of accuracy. In comparison, the modified FV method can attain fourth order of accuracy. But we observe that the convergence rate of the modified FV method is more than fourth order because of the interaction between the conversion formula and the 1D reconstruction. One can conclude that the numerical results completely achieve the theoretically expected order of accuracy.

4.2.2 Shock/mixing layer interaction

We test the performance of our modified FV method for the interactions between shock waves and shear layers (Yee et al. 1999; Lo et al. 2010).

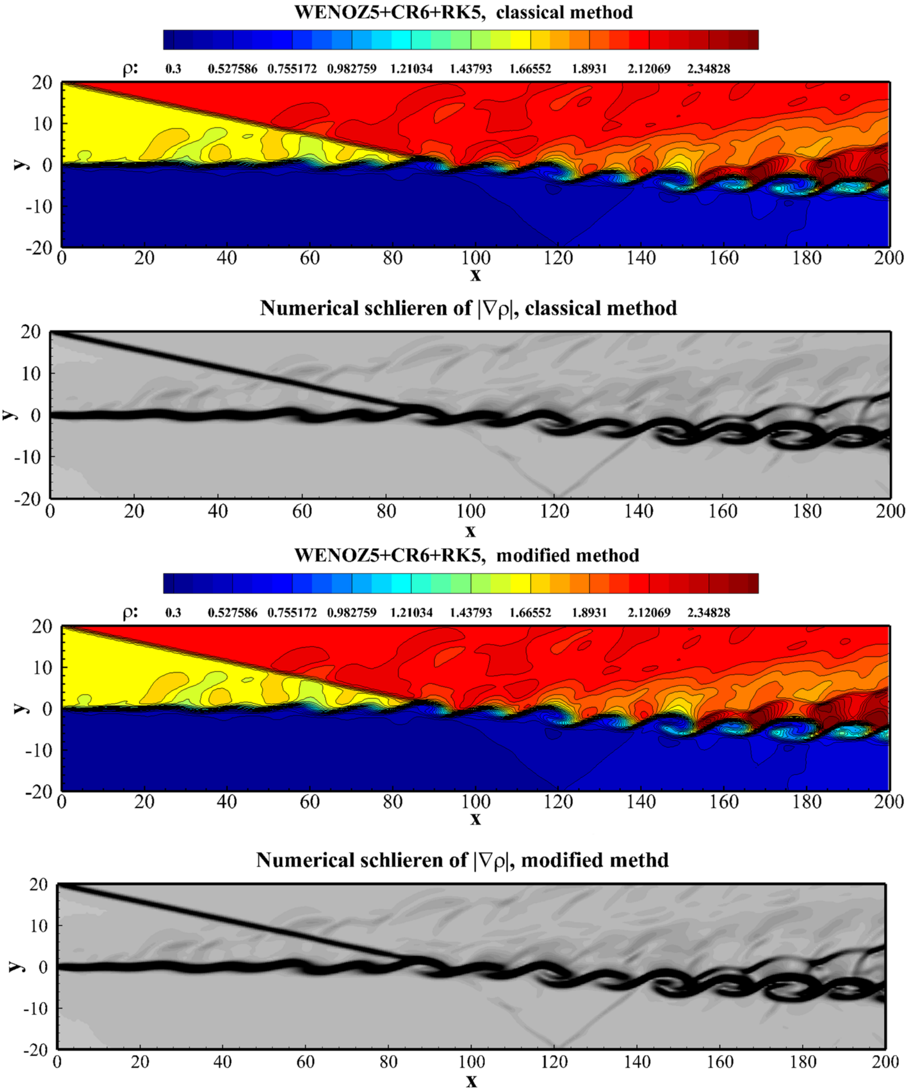

Fig. 3 Comparison of the classic method with the modified method for shock/mixing layer interaction problem at $T = 120$ on the 400×80 grid. Density contours and numerical schlieren $|\nabla \rho|$ are shown, and WENOZ5 and sixth-order central reconstructions (CR6) as well as RK5 are used in both methods

A spatially developing mixing layer has an initial convective Mach number of 0.6, and a 12° oblique shock originating from the upper-left corner interacts with the vortices developed from the instability of the shear layer. The initial conditions are given in Table 3.2 of Yee et al. (1999). The oblique shock is refracted by the shear layer and then reflects from the bottom slip wall, and transmits the shear layer again. To avoid boundary layer formation, the lower wall uses a slip condition, the upper boundary condition is taken from the flow states behind the oblique shock, and the outflow boundary is arranged to be supersonic.

The inflow boundary condition has a velocity profile with fluctuations,

$$v_1 = 2.5 + 0.5\tanh(2y), \quad v_2 = v_2',$$
$$v_2' = \sum_{k=1}^{2} a_k \cos(2\pi kt/\tau + \phi_k)\exp(-y^2/b) \tag{4.16}$$

with period $\tau = \lambda/u_c$, wavelength $\lambda = 30$, and convective velocity $u_c = 2.68$. Other constants are $a_1 = a_2 = 0.05$, $\phi_1 = 0$, $\phi_2 = \pi/2$ and $b = 10$. The Prandtl number Pr = 0.72, and the Reynolds number Re $= 500$. This case was run on a $[0, 200] \times [-20, 20]$ domain with a 400×80 uniform grid, and the finial output time is $t = 120$.

Figure 3 shows the density contours and numerical Schlieren $|\nabla\rho|$ for this example computed using the two different methods. We can observe that the shock makes the bulk of the vortices shift towards the lower side due to high pressure after the shock. The results computed by the two methods are in good agreement with other simulations (Yee et al. 1999; Lo et al. 2010). We also see that the modified method has almost the same resolution as the classical method on the uniform grid, which suggests that the conversion formulas do not cause any numerical difficulty for the interactions of shock wave and shear layer.

5 Conclusions

We have extended the modified dimension-by-dimension finite-volume method on Cartesian grids to nonlinear convection–diffusion equations. The present modified finite-volume (FV) method uses one-dimensional central reconstruction of conservative variables for diffusion terms. Fourth-order conversions between edge-averaged values and edge center values of the conservative variables, their gradients and viscous fluxes guarantee that edge-averaged numerical viscous fluxes have fourth-order accuracy. Moreover, it only needs one flux evaluation per grid cell interface such that the method is slightly more expensive than the classical dimension-by-dimension FV method. The numerical tests show that the modified FV method achieves the expected order of accuracy when applied to smooth nonlinear convection–diffusion problems and is robust for calculating non-smooth nonlinear problems like shock/mixing layer interaction. The proposed modified FV method on Cartesian grids is suitable for high-order accurate numerical simulation of viscous shocked flows.

Acknowledgements This work is supported by Natural Science Foundation of China (91641107, 91852116), and Fundamental Research of Civil Aircraft (MJ-F-2012-04).

Conflict of interest The authors declare that they have no conflict of interest to this work.

References

Angermann L, Wang S (2019) A super-convergent unsymmetric finite volume method for convection-diffusion equations. J Comput Appl Math 358:179–189. https://doi.org/10.1016/j.cam.2019.03.017

Blazek J (2005) Computational fluid dynamics: principles and applications, 3rd edn. Butterworth Heinemann of Elsevier, Oxford. https://doi.org/10.1016/C2013-0-19038-1

Borges R, Carmona M, Costa B, Don WS (2008) An improved weighted essentially non-oscillatory scheme for hyperbolic conservation laws. J Comput Phys 227(6):3191–3211. https://doi.org/10.1016/j.jcp.2007.11.038

Buchmüller P, Helzel C (2014) Improved accuracy of high-order WENO finite volume methods on Cartesian grids. J Sci Comput 61:343–368. https://doi.org/10.1007/s10915-014-9825-1

Buchmüller P, Dreherb J, Helzel C (2016) Finite volume WENO methods for hyperbolic conservation laws on Cartesian grids with adaptive mesh refinement. Appl Math Comput 272:460–478. https://doi.org/10.1016/j.amc.2015.03.078

Buchmüller P, Dreherb J, Helzel C (2018) Improved accuracy of high-order WENO finite volume methods on Cartesian grids with adaptive mesh refinement. Math Stat 236:263–272. https://doi.org/10.1007/978-3-319-91545-6_21

Chana J, Evans JA, Qiu W (2014) A dual Petrov-Galerkin finite element method for the convection–diffusion equation. Comput Math Appl 68:1513–1529. https://doi.org/10.1016/j.camwa.2014.07.008

Cheichan MS, Kashkool HA, Gao F (2019) A weak Galerkin finite element method for solving nonlinear convection–diffusion problems in two dimensions. Appl Math Comput 354:149–163. https://doi.org/10.1016/j.amc.2019.02.043

Chou CS, Shu CW (2007) High order residual distribution conservative finite difference WENO schemes for convection–diffusion steady state problems on non-smooth meshes. J Comput Phys 224:992–1020. https://doi.org/10.1016/j.jcp.2006.11.006

Cui X, Yuan GW, Yue JY (2016) Numerical analysis and iteration acceleration of a fully implicit scheme for nonlinear diffusion problem with second-order time evolution. Numer Methods Partial Differ Equ 32:121–140. https://doi.org/10.1002/num.21988

Don WS, Borges R (2013) Accuracy of the weighted essentially non-oscillatory conservative finite difference schemes. J Comput Phys 250:347–372. https://doi.org/10.1016/j.jcp.2013.05.018

Du YL, Yuan L, Wang YH (2019) A high-order modified finite volume WENO method on 3D Cartesian grids. Commun Comput Phys 26:768–784. https://doi.org/10.4208/cicp.OA-2018-0254

Gao Y, Liang D, Li Y (2019) Optimal weighted upwind finite volume method for convection–diffusion equations in 2D. J Comput Appl Math 359:73–87. https://doi.org/10.1016/j.cam.2019.03.018

Gassner G, Lörcher F, Munz CD (2008) A discontinuous Galerkin scheme based on a space-time expansion II: viscous flow equations in multi dimensions. J Sci Comput 34:260–286. https://doi.org/10.1007/s10915-007-9169-1

Golbabai A, Arabshahi MM (2010) A numerical method for diffusion–convection equation using high-order difference schemes. Comput Phys Commun 181:1224–1230. https://doi.org/10.1016/j.cpc.2010.03.008

Huang Z, Lin G, Ardekani AM (2019) A mixed upwind/central WENO scheme for incompressible two-phase flows. J Comput Phys 387:455–480. https://doi.org/10.1016/j.jcp.2019.02.043

Liang D, Zhao W (2006) An optimal weighted upwind covolume method on non-standard grids for convection–diffusion problems in 2D. Int J Numer Meth Eng 67:553–577. https://doi.org/10.1002/nme.1641

Lin Y, Gao X, Xiao MQ (2009) A high-order finite difference method for 1D nonhomogeneous heat equations. Numer Methods Partial Differ Equ 25:327–346. https://doi.org/10.1002/num.20345

Lo SC, Blaisdell GA, Lyrintzis AS (2010) High-order shock capturing schemes for turbulence calculations. Int J Numer Meth Fluids 62:473–498. https://doi.org/10.1002/fld.2021

Manzini G, Russo A (2008) A finite volume method for advection-diffusion problems in convection-dominated regimes. Comput Methods Appl Mech Eng 197:1242–1261. https://doi.org/10.1016/j.cma.2007.11.014

Morton KW (1996) Numerical solution of convection–diffusion problems. Chapman & Hall, London. https://doi.org/10.1201/9780203711194

Schmidmayer K, Petitpas F, Daniel E (2019) Adaptive mesh refinement algorithm based on dual trees for cells and faces for multiphase compressible flows. J Comput Phys 388:252–278. https://doi.org/10.1016/j.jcp.2019.03.011

Shu CW (1997) Essentially non-oscillatory and weighted essentially non-oscillatory schemes for hyperbolic conservation laws. NASA/CR-97-206253, ICASE Report NO. 97-65

Sun HW, Li LZ (2014) A CCD-ADI method for unsteady convection–diffusion equations. Comput Phys Commun 185:790–797. https://doi.org/10.1016/j.cpc.2013.11.009

Sun Y, Wang ZJ, Liu Y (2006) Spectral (finite) volume method for conservation laws on unstructured grids VI: extension to viscous flow. J Comput Phys 215:41–58. https://doi.org/10.1016/j.jcp.2005.10.019

Tamaki Y, Imamura T (2017) Efficient dimension-by-dimension higher order finite-volume methods for a Cartesian grid with cell-based refinement. Comput Fluids 144:74–85. https://doi.org/10.1016/j.compfluid.2016.12.002

Teng F, Yuan L, Tang T (2011) A speed-up strategy for finite volume WENO schemes for hyperbolic conservation laws. J Sci Comput 46:359–378. https://doi.org/10.1007/s10915-010-9407-9

Tian J (2019) An upwind finite volume method for convection–diffusion equations on rectangular mesh. Chaos Solitons Fractals 118:159–165. https://doi.org/10.1016/j.chaos.2018.09.011

Titarev VA, Toro EF (2004) Finite-volume WENO schemes for three-dimensional conservation laws. J Comput Phys 201:238–260. https://doi.org/10.1016/j.jcp.2004.05.015

Vevek US, Zang B, New TH (2019) Adaptive mapping for high order WENO methods. J Comput Phys 381:162–188. https://doi.org/10.1016/j.jcp.2018.12.034

Wang X, Li Z (2007) Dynamics for a type of general reaction–diffusion model. Nonlinear Anal 67:2699–2711. https://doi.org/10.1016/j.na.2006.09.034

Wang H, Liang D, Ewing RE, Lyons SL, Qin G (2000) An approximation to miscible fluid flows in porous media with point sources and sinks by an Eulerian- Lagrangian localized adjoint method and mixed finite element methods. SIAM J Sci Comput 22:561–581. https://doi.org/10.1137/S1064827598349215

Xie J, Zhang Z (2018) The high-order multistep ADI solver for two-dimensional nonlinear delayed reaction–diffusion equations with variable. Comput Math Appl 75:3558–3570. https://doi.org/10.1016/j.camwa.2018.02.017

Yee HC, Sandham ND, Djomehri MJ (1999) Low-dissipative high-order shock-capturing methods using characteristic-based filters. J Comput Phys 150:199–238. https://doi.org/10.1006/jcph.1998.6177

Yue H, Cheng J, Liu T (2017) A symmetric direct discontinuous Galerkin method for the compressible Navier–Stokes equations. Commun Comput Phys 22:375–392. https://doi.org/10.4208/cicp.OA-2016-0080

Zhang T, Chen Y (2019) An analysis of the weak Galerkin finite element method for convection–diffusion equations. Appl Math Comput 346:612–621. https://doi.org/10.1016/j.amc.2018.10.064

Zhang S, Shu CW (2007) A new smoothness indicator for the WENO schemes and its effect on the convergence to steady state solutions. J Sci Comput 31:273–305. https://doi.org/10.1007/s10915-006-9111-y

Zhang R, Zhang M, Shu CW (2011) On the order of accuracy and numerical performance of two classes of finite volume WENO schemes. Commun Comput Phys 9(3):807–827. https://doi.org/10.4208/cicp.291109.080410s